Journal of Statistical Physics, Vol. 69, Nos. 5/6, 1992

Monte Carlo Simulation of the Two-Dimensional Planar Model

Chris Bowen,[1] D. L. Hunter,[1] and Naeem Jan[1]

Received July 30, 1991; final July 9, 1992

We present results for the two-dimensional planar model on the square lattice. We have developed a Monte Carlo routine which is more efficient than the single-spin-flip algorithms used previously. We report on the variation of the following quantities with temperature: specific heat, energy, magnetization, susceptibility, correlation function, helicity modulus, the density of vortex/antivortex pairs, the average distance between a vortex and its nearest antivortex, and the average distance between a vortex/antivortex pair and the nearest pair. Our results are in excellent agreement with the reliable results reported in the literature and are in accord with the general features of the Kosterlitz–Thouless theory.

KEY WORDS: Planar magnetic model; critical phenomena; Kosterlitz–Thouless transition; vortices.

1. INTRODUCTION

The planar model and its closely related cousin the xy model show unique features at low temperatures.[1] The planar model consists of spins of unit dimension which are restricted to a plane, whereas in the xy model the spins are three-dimensional vectors. These spins populate a lattice which in this work is the two-dimensional (2D) square. These models have been used as a means of theoretically studying thin-film superfluids, thin-film superconductors, arrays of Josephson junctions, and dirty superconductors[2] and we consider the planar model as an appropriate starting point for a proper understanding of high-T_c superconductors.[3] The Hamiltonian for these models consists of interactions $J_x = J_y$ and $J_z = 0$.

[1] Physics Department, St. Francis Xavier University, Antigonish, Nova Scotia, Canada B2G 1C0.

0022-4715/92/1200-1097$06.50/0

A theorem due to Mermin and Wagner[4–6] states that there should be no long-range order for a system with a spin dimensionality $\geqslant 2$ and a system dimensionality $\leqslant 2$, conditions satisfied by the 2D planar model. However the early series expansion results of Stanley and Kaplan[7–9] indicate the onset of some type of phase transition despite the lack of long-range order expected for a typical phase transition. In this paper we focus on the planar model whose Hamiltonian is

$$\begin{aligned} H\{\sigma\} &= -J_{ij} \sum_{\langle ij \rangle} (\overline{\sigma_i} \cdot \overline{\sigma_j}) \\ &= -J_{ij} \sum_{ij} (\sigma_{ix}\sigma_{jx} + \sigma_{iy}\sigma_{jy}) \\ &= -J_{ij} \sum_{ij} \cos(\theta_i - \theta_j) \end{aligned} \tag{1}$$

The spin–spin correlation function $\langle \sigma_0 \sigma_r \rangle$ for a system with a *conventional* second-order phase transition[10] shows the following behavior in the different temperature regimes.

For temperatures greater than the critical temperature T_c we expect

$$\lim_{r \to \infty} \langle \sigma_0 \sigma_r \rangle = 0 \tag{2a}$$

while for temperatures less than the critical temperature

$$\lim_{r \to \infty} (\sigma_0 \sigma_r) = m^2 \tag{2b}$$

where m is the spontaneous magnetization or order parameter.

However, at T_c the correlation function is expected to show a power law decay of the form

$$\langle \sigma_0 \sigma_r \rangle \sim r^{-(d-2+\eta)} \tag{2c}$$

where d is the dimensionality of the system and η is the correlation function exponent.

We may appreciate the unique nature of the phase transition in the planar model by considering the Gaussian approximation,[1,11–13] which is considered to be reliable at low temperatures. This is

$$H = \tfrac{1}{2} \int (\nabla \theta)^2 \tag{3}$$

The Gaussian approximation of the planar model predicts that for all temperatures

$$\langle \sigma_0 \sigma_r \rangle \sim r^{-T/2\pi} \tag{4}$$

whereas the susceptibility χ is infinite for all temperatures $T < 8\pi$. Although the Gaussian approximation is crude, it offers some indication of the rather peculiar behavior of the low-temperature phase of the planar model. Thus we find agreement with the theorem of Mermin and Wagner in that there is no long-range order, but we observe a power-law decay of the correlation function over a wide range of temperatures, behavior usually expected only at the critical point.

The next section is devoted to a brief review of the Kosterlitz–Thouless (KT) theory followed by a review of the standard Monte Carlo routine. We describe our modifications to this procedure. In the subsequent sections we present our results and compare with the results of others (some obtained with the aid of supercomputers and novel tricks such as generalization of the Swendsen–Wang multi-spin-flip approach).[14,15] Our results confirm the general scenario of the KT theory. In particular, we observe that the vortex/antivortex pair starts to unbind at a temperature approximately close to the KT temperature and that the vortices are more or less free at a temperature comparable to the observed peak of the specific heat.

2. KOSTERLITZ–THOULESS THEORY

Our understanding of the planar model is embodied in what is commonly referred to as the Kosterlitz–Thouless (KT) theory,[1,16,17] which we briefly summarize. These is no long-range order at any finite temperatures, so that the magnetization is always 0 for $T > 0$. At low temperatures the system is unstable to spin waves and the Gaussian approximation is a good description since it is most probable that neighboring spins are more or less aligned in the same direction. In this low-temperature phase, KT predicts a power-law decay of the correlation function given by Eq. (2c) but with the distinction that $\eta(T)$ is temperature dependent. As the temperature is increased, additional spin excitations in the form of vortices are created. The presence of vortices causes deviations toward larger values for the correlation function exponent η, which the Gaussian approximation estimates to be $T/2\pi$. The presence of the vortices may be viewed as producing an effective temperature increase to the Gaussian result. The energy of a solitary vortex is proportional to the logarithm of the linear size of the system and it is energetically favourable to form pairs. As the temperature is increased, bound vortex/antivortex pairs are formed in addition to the spin waves. At a specific temperature which is referred to as the KT transition temperature the vortex pairs start to dissociate. At a somewhat higher temperature all the vortex pairs become for the first time weakly bound and this is reflected by a peak in the specific heat. There is

a clear distinction between the KT transition and the peak of the specific heat. Above the KT transition temperature, the correlation function changes from exhibiting a power-law decay to an exponential decay given by the equation

$$\langle \sigma_0 \sigma_r \rangle \sim e^{-r/\xi} \tag{5}$$

where ξ is defined as the correlation length.

The susceptibility is infinite for all temperatures below the KT temperature and is expected to diverge with the correlation length as

$$\chi \sim \xi^{2-\eta(T)} \tag{6}$$

where KT predicts that $\eta(T_c) = 1/4$.

Above the KT transition the susceptibility and the correlation length are expected to diverge with an essential exponential singularity as

$$\begin{aligned} \chi &= a_\chi e^{b_\chi t^{-\nu}} \\ \xi &= a_\xi e^{b_\xi t^{-\nu}} \end{aligned} \tag{7}$$

where t is the reduced temperature $[t \equiv (T - T_c)/T_c]$ and the exponent $\nu = 1/2$, as predicted by KT theory.

3. MONTE CARLO MECHANICS

The Monte Carlo method is comprehensively reviewed in ref. 18 and we briefly review the important elements for the planar model.[19–21] Start with an initial state of the spins—random directions if the starting temperature is high ($kT/\mathrm{J} \sim 2.0$) or all spins ordered if the starting temperature is low ($kT/\mathrm{J} \sim 0.2$) and, for a continuous temperature scan, the initial configuration is the last output configuration from the previous temperature. The micro unit of a Monte Carlo step is as follows:

(i) The random selection is made of a site on the lattice—we shall refer to the spin at this site as the target spin.

(ii) The energy is obtained from the interactions of the target spin with its four nearest neighbors.

(iii) A new direction for the target spin is randomly selected and the energy for this new orientation is evaluated.

(iv) The selection between the two orientations of the target spin is made using their Boltzmann probabilities.

When every site has been interrogated and updated in this way we have completed a Monte Carlo step. Several thousand Monte Carlo time steps are performed before the system is expected to reach equilibrium and then hundreds of thousands of configurations are generated in order to obtain reliable equilibrium statistics. A useful reference is the article by Tobochnik and Chester,[19] where sufficient details and results are supplied to allow for an easy check of the algorithm. A weakness with the above Monte Carlo scheme is the random selection of the new orientation of the target spin, as it is unlikely that we would select a probable direction in this manner unless many attempts have been made in the selection of possible directions. This places severe computational demands on obtaining reliable equilibrium data and we address this problem next.

The resultant vector R obtained from summing the four neighboring spins of the target spin has a magnitude $0 < R < 4$. We discretized R into intervals of 0.025. Thus a value of R which is between 0.0125 and 0.0375 we consider as 0.025. For each value of R we construct a table of angles $\{\Theta_i\}$ consisting of 4000 entries where the probability of an angle Θ is proportional to its Boltzmann probability $[\exp([J/kT] * R\cos\Theta)]$. The angle Θ is the deviation from the resultant direction. This table is refreshed at periodic intervals during a Monte Carlo run—after every 5000 Monte Carlo steps. Whenever we visit a site we select a new direction which is dependent on the resultant vector from the nearest neighbors of the target spin (properly discretized). This new angle is obtained by simply generating a random number in the interval 0–4000. We may get a rough estimate of the improvements generated by this procedure by considering a visit to a single site as comparable to several visits from the standard approach. The table of angles may be constructed from 4000 visits (we do not claim that our approach is 4000 times better, but only that we select an angle for an update from 4000 angles) by the standard method and the frequency of an angle in the table is proportional to its Boltzmann weight. "Important sampling" is used to select the new state of the target spin. Preliminary tests on a DEC workstation indicate that our approach is about 8 μsec faster in updating a single spin. A check of a deep quench from an initial random state to $T = 0.3$ shows that this method relaxes to the equilibrium energy in about 300 MCS, while the standard approach took about 12,000 MCS (Fig. 1). The differences in efficiency between the two methods will be indistinguishable at high temperatures and both methods will suffer from critical slowing down near T_c. The update to a new state takes only slightly longer than the update of an Ising spin. This difference is due to the evaluation of the resultant vector, whereas for the Ising model we simply sum a set of $+1$'s and -1's. We have checked the effects of minimizing the interval of discretization and find the Monte Carlo data to be

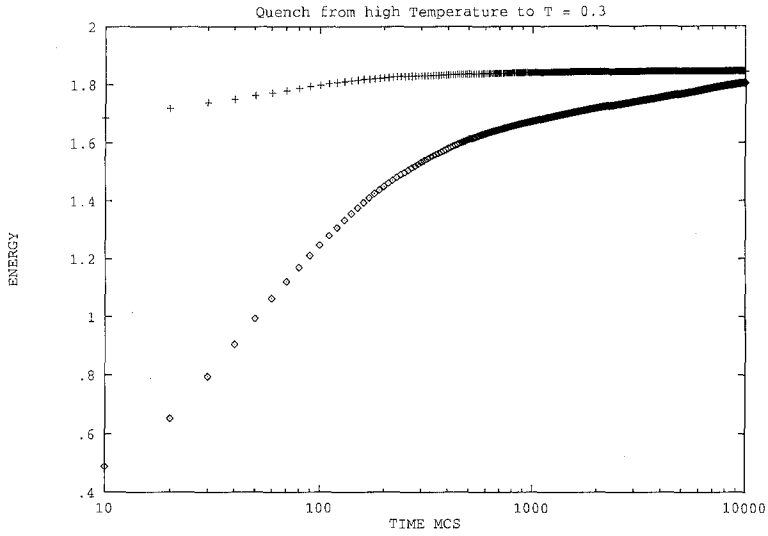

Fig. 1. Time evolution of the energy of the system from an initial random state to equilibrium at $T=0.3$. Note that the standard method $(\cdot)$ is still not at equilibrium after 10,000 MCS, while the modified method $(+)$ has attained equilibrium after ~ 300 MCS.

indistinguishable from those obtained using the above constraint. We show these results below and also compare our thermodynamic averages with the results obtained with other techniques.[14,15,22,23]

4. RESULTS

The energy of a 30×30 system versus temperature is shown in Fig. 2a, where we include the results of Tobochnik and Chester[19] $(\cdot)$ and those of Fernandez *et al.*[22] $(+)$. The agreement is good. The fluctuation of the energy is a measure of the specific heat and this is shown in Fig. 2b. We are interested in the variation of the peak of the specific heat with system size and this is shown in Fig. 3a, where the peak of the specific heat is plotted versus $1/L$ (the linear dimension of the system). We took advantage of the histogram method highlighted by Ferrenberg and Swendsen[24] and the modifications made to this technique by Bowen *et al.*[25] to reduce computational demands. It seems from this extrapolation that the peak of the specific heat for the infinite system will occur at $T \sim 1.02 \pm 0.02$. The other property worth noting from Fig. 3b is that the height of the specific heat peak is more or less independent of the system size for $L > 30$. The extrapolated temperature at which the peak of the specific heat occurs for

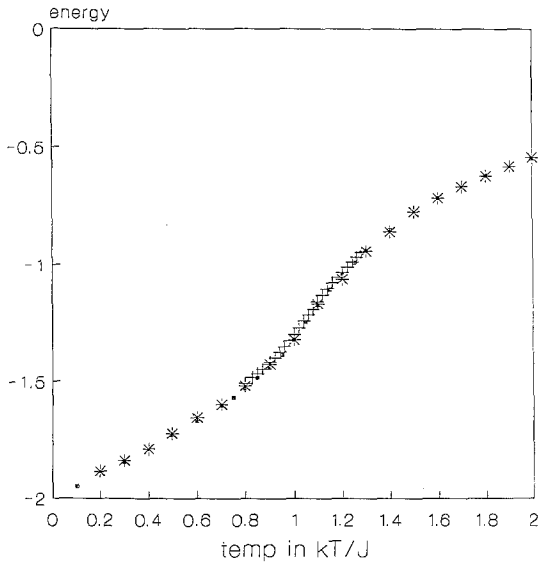

(a)

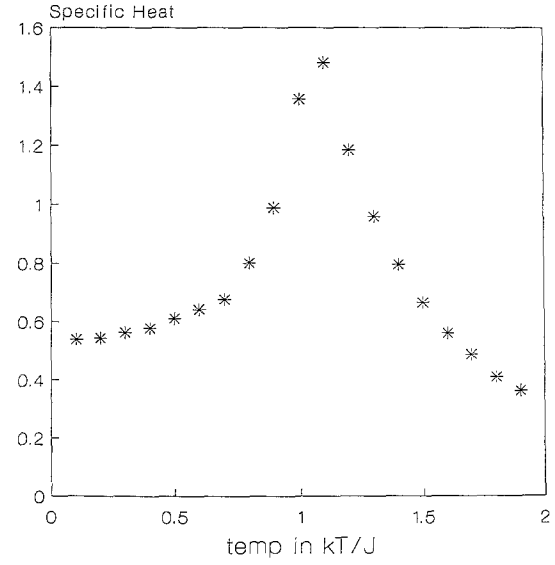

(b)

Fig. 2. Monte Carlo data for an $L = 30$ system. (a) The energy vs. temperature (*) with the results of Tobochnik and Chester[19] (·) and Fernandez *et al.*[22] (+) superimposed for comparison; (b) the specific heat measured from energy fluctuations vs. temperature; a peak is observed at $\sim 1.07kT/J$.

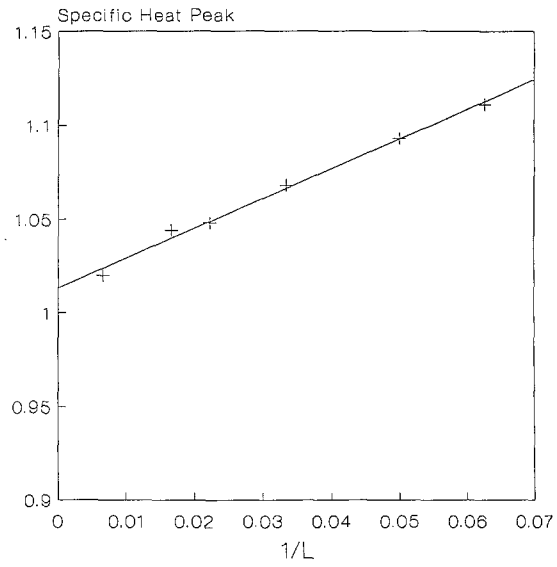

Fig. 3. (a) The specific heat peak temperature vs. the inverse linear dimension of the system $(1/L)$. The extrapolation for an infinite system gives a peak at about $T = 1.02kT/J$. (b) The specific heat vs. temperature for $L = 20$ $(\cdot)$, $L = 30$ $(+)$, $L = 45$ $(*)$, and $L = 60$ $(\square)$. The height of the peak is independent of system size for $L > 30$.

the infinite system agrees with the results of Tobochnik and Chester[19] and Gupta *et al.*[23]

The helicity modulus[26] is defined by

$$\gamma = -\frac{1}{2}\langle E\rangle - \frac{J}{k_B T L^2}\left\langle \left[\sum_{\langle ij\rangle} \sin(\theta_i - \theta_j)\,\bar{e}_{ij}\cdot\bar{x}\right]^2\right\rangle \tag{8}$$

where $\mathbf{e}_{ij}$ is a unit vector pointing from the target spin i to the nearest neighbor j and $\mathbf{x}$ is a unit vector pointing along the x axis in the plane of the lattice. The helicity modulus is a measure of the relative phase shift of the spins of the system. For an infinite system, it is expected to show a discontinuous drop as the temperature approaches T_c, becoming 0 for $T > T_c$. For the finite system, we observe an effective T_c by looking for the intersection of a straight line (---) of slope $2/\pi$ with the helicity modulus curve. This occurs at the temperature of 0.91, as shown in Fig. 4. This result is in good agreement with that reported in the literature. We also looked at the helicity modulus for the 60×60 system and note that T_c is now 0.905. The critical temperature is only weakly dependent on system size and the value appears to be ~ 0.90, in agreement with the value of $T_c = 0.89$ quoted by Tobochnik and Chester.[19] This excludes the peak of the specific heat from being associated with T_c, so that we confirm that the specific heat peak is unrelated to critical phenomena.

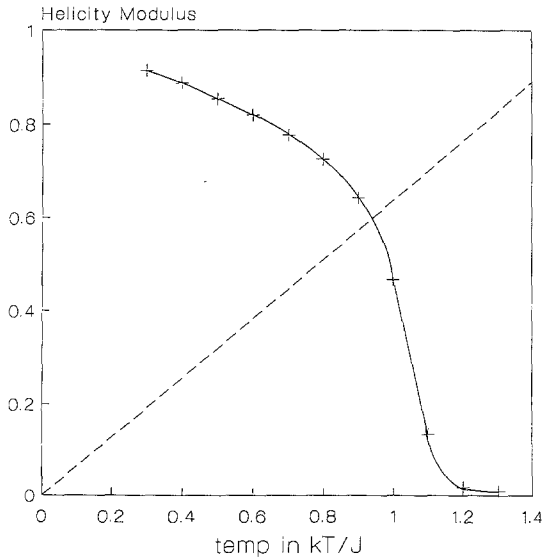

Fig. 4. A plot of the helicity modulus vs. temperature for an $L = 30$ system. The intersection of $2T/\pi$ with the curve gives a measurement of $T_c \sim 0.91kT/J$.

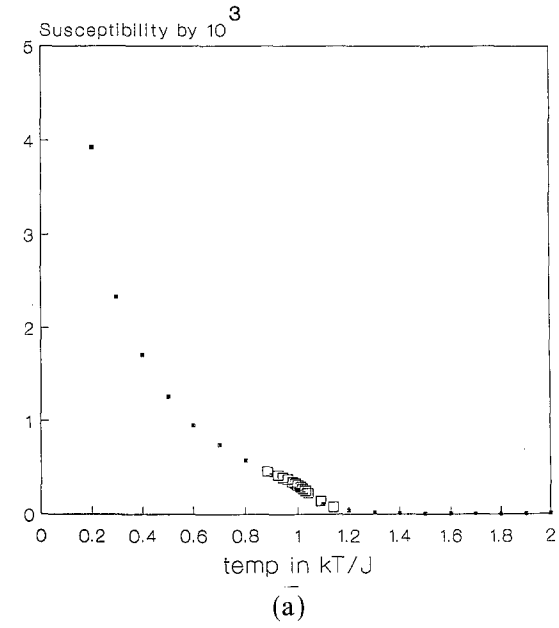

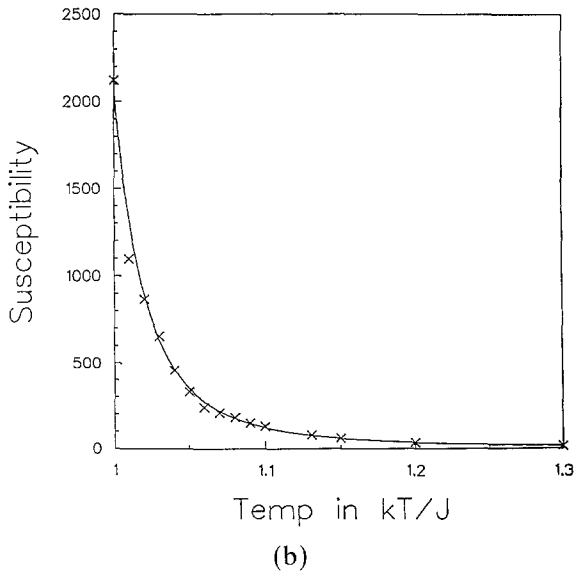

Fig. 5. (a) The susceptibility vs. temperature (·) for an $L = 30$ system with the results of Edwards[15] (□) for an $L = 32$ system superimposed. (b) Susceptibility vs. temperature for $T > T_c$. The solid line shows the prediction of KT theory.

The fluctuations of the magnetization determine the susceptibility χ, and the variation of the susceptibility with temperature is shown in Fig. 5a, where we include the data of Edwards.[15] The agreement is good. The variation of χ for temperatures above the KT transition is shown in Fig. 5b. The solid line is the prediction of the KT theory with the following values for the constants in Fig. (7): $a_\chi = 0.135$, $b_\chi = 3.21$, $\nu = 1/2$, and $T_c = 0.90$. We do not think that our data are of sufficient accuracy, mainly due to the relatively small system size, to resolve the conflict in the literature between the exponential singularity prediction of KT and the normal power-law behavior of a second-order transition.[23,27] The spin–spin correlation function critical exponent η is expected to vary with temperature for temperatures below T_c according to Eq. (2c) and this is shown in Fig. 6. We note in Table I that at low temperatures $\eta(T)$ is in excellent agreement with the predictions of spin-wave theory. At the critical temperature of 0.90 we measure a value for η of ~ 0.23, which is close to the KT prediction of 0.25.

The density of the vortex/antivortex pairs as a function of temperature is shown in Fig. 7a, and in Fig. 7b we show the ln of the density versus temperature. The slope of the graph gives the energy to create a vortex/

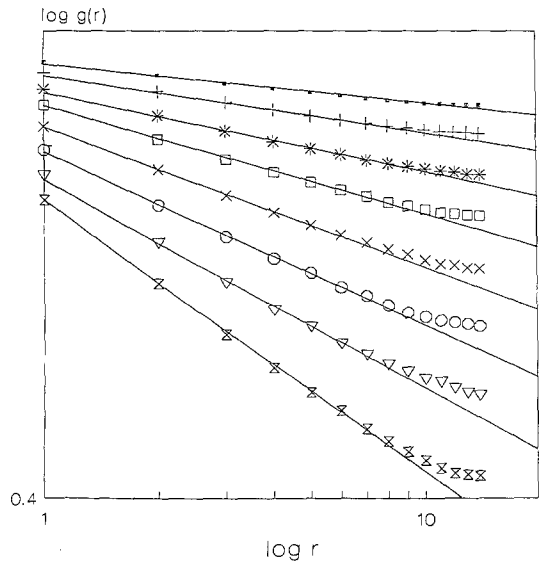

Fig. 6. A log-log plot of the correlation function vs. distance r. Shown are plots for an $L = 30$ system for $T = 0.2$ ($\cdot$), $T = 0.3$ ($+$), $T = 0.4$ ($*$), $T = 0.5$ ($\square$), $T = 0.6$ ($\times$), $T = 0.7$ ($\bigcirc$), $T = 0.8$ ($\triangledown$), and $T = 0.9$ ($\times$). The values of η obtained from the slopes are listed in Table I along with the predictions from the spin-wave theory (in parentheses).

antivortex pair to be ~ 7.4. This value is to be compared with 9.4 of TC and 10.2 from KT. In Fig. 8a we show the thermal average separation of a vortex with its nearest antivortex (+). At low temperatures we observe a tightly bound pair where the vortex and its bound neighbor are on neighboring plaquettes. At a temperature of ~ 0.9 we observe the beginning of a separation of their pair, reaching a maximum at around $T \sim 1.1$. Above this temperature, increased crowding from the high V/AV pair density begins to reduce the V/AV separation. We also include the average distance between a V/A pair and the next closest pair (·). We note that at low temperatures the pairs are widely separated, indicating a low density of V/A pairs. However, as we approach a temperature of ~ 1.2, the distance between two pairs and the V/AV separation become of the same order, indicating the complete unbinding of the vortex pairs into a vortex gas. Figure 8b shows this vortex pair uncoupling more clearly by showing the

Table I. Monte Carlo Data for the $L = 30$ System[a]

T	Energy	χ	η	Vorticity	D	R	Helicity modulus
0.1	−1.9495	8829	—	0	—	—	0.9745
0.2	−1.8976	4416	0.035(0.032)	0	—	—	0.9478
0.3	−1.8438	2982	0.051(0.048)	0	—	—	0.9195
0.4	−1.7877	2241	0.071(0.064)	1.89E−7	1.000	1311	0.8892
0.5	−1.7297	1799	0.092(0.080)	6.98E−6	1.043	214	0.8567
0.6	−1.6682	1497	0.12 (0.095)	7.52E−5	1.052	65.1	0.8204
0.7	−1.6022	1266	0.15 (0.111)	4.11E−4	1.099	27.8	0.7779
0.8	−1.5277	1113	0.18 (0.127)	0.00153	1.165	14.4	0.7201
0.9	−1.4402	995	0.23 (0.143)	0.00446	1.293	8.45	0.6239
1.0	−1.3278	899	—	0.01110	1.569	5.36	0.4119
1.1	−1.1808	817	—	0.02384	2.003	3.65	0.0788
1.2	−1.0473	749	—	0.03742	2.101	2.92	0.0043
1.3	−0.9397	692	—	0.04934	2.053	2.54	0.0024
1.4	−0.8528	643	—	0.05956	2.000	2.31	—
1.5	−0.7784	600	—	0.06869	1.952	2.15	—
1.6	−0.7171	562	—	0.07643	1.917	2.04	—
1.7	−0.6649	529	—	0.08313	1.886	1.96	—
1.8	−0.6192	500	—	0.08908	1.859	1.89	—
1.9	−0.5811	474	—	0.09406	1.840	1.84	—

[a] Temperature listed in column 1, energy in column 2, susceptibility in column 3, η from the low-temperature form of the spin correlation function given by Eq. (2c) in column 4 along with the spin-wave prediction ($\eta = T/2\pi$) in parentheses, vortex pairs/site/MC step in column 5, average vortex–antivortex separation D in column 6, average separation between a V/AV pair and its nearest pair R in column 7, and helicity modulus in column 8.

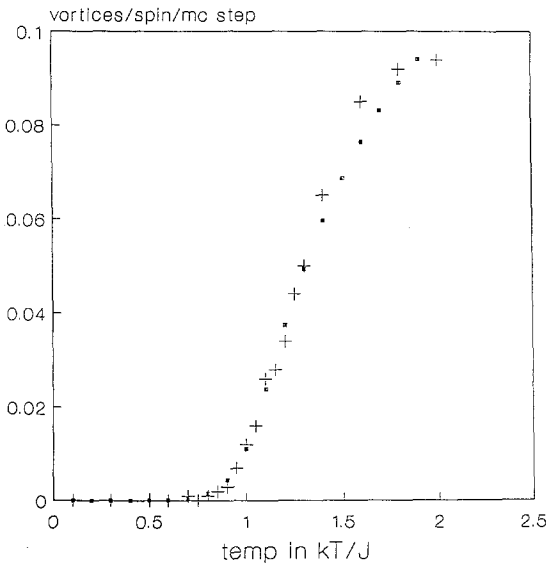

(a)

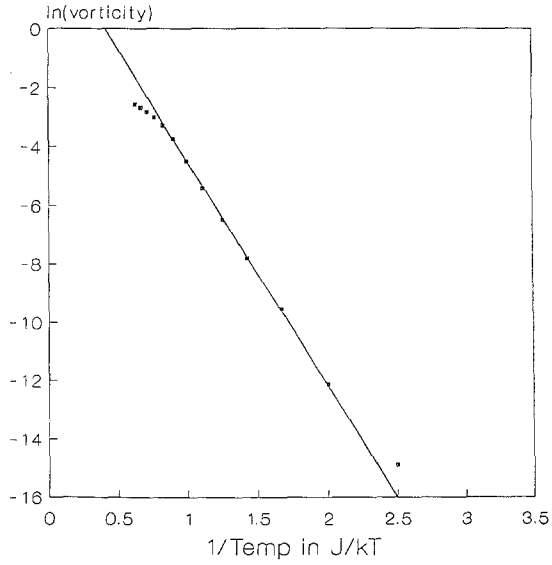

(b)

Fig. 7. (a) Plot of the vorticity/site vs. temperature (·) for an $L = 30$ system with the values of Tobochnik and Chester[19] included for comparison (+). (b) A plot of ln (vorticity) vs. the inverse temperture gives the energy (7.4) to create a V/AV pair.

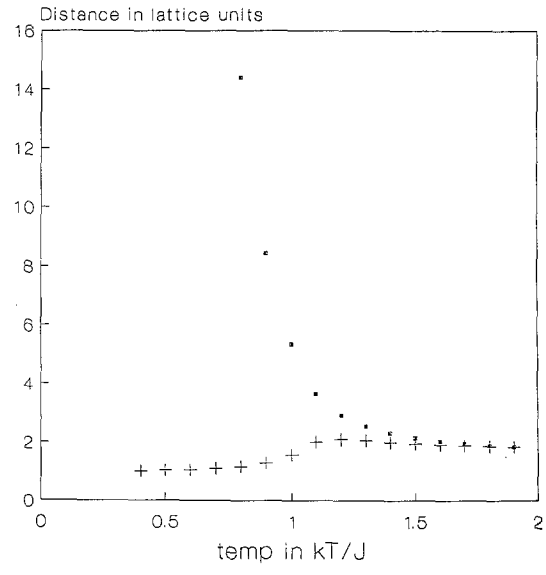

(a)

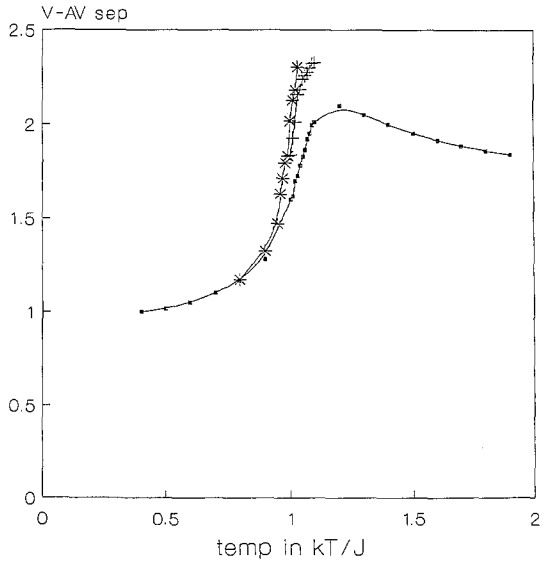

(b)

Fig. 8. Monte Carlo results for (a) an $L = 30$ system showing D, the V–AV separation (+), and R, the average pair–pair separation (·). At T_c the pairs begin to dissociate into a vortex gas; at $T = 1.2$, D and R are of the same order. (b) The V–AV separation for $L = 30$ (·), $L = 64$ (+), and $L = 100$ (*), where a shift occurs in the maximum separation toward a lower temperature.

V/AV separation versus temperature through the KT transition temperature. Several curves are shown representing different lattice sizes. We see that the V/AV pair separation reaches a maximum at a somewhat lower temperature closer to the KT transition temperature for larger lattice sizes. These peaks reflect the point at which the V/AV pairs are weakly bound and the slight shift in the peak with system size is consistent with the observed shift in the specific heat peak with system size.

Below the KT transition the correlation length is infinite and this is reflected in the power-law decay of the correlation function. Above T_c the spin–spin correlation function is expected from scaling arguments to decay as[28]

$$g(r) \equiv \langle \sigma_0 \sigma_r \rangle \simeq (1/r^{1/4})\, F(r/\xi) \tag{9}$$

where $F(x)$ is a universal crossover function with $x \equiv r/\xi$. Figure 9 shows this function for $T = 1.05$ ($\xi = 15.0$), $T = 1.07$ ($\xi = 13.0$), and $T = 1.1$ ($\xi = 9.6$). The limiting behavior of $F(x)$ is

$$\begin{aligned} F(x) &\approx (\ln x)^{1/8} \qquad x \ll 1 \\ &\approx x^{-1/4} e^{-x} \qquad x \gg 1 \end{aligned} \tag{10}$$

We have assumed the large-x behavior of $F(x)$ in our determination of the correlation length ξ.

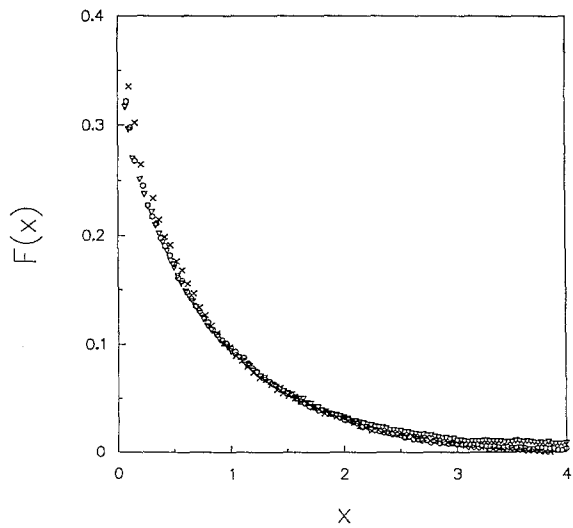

Fig. 9. Monte Carlo results for an $L = 151$ system of the universal crossover function $F(x)$ vs. x, where $x = r/\xi$. The plot shows the function at $T = 1.05$ (∇), $T = 1.07$ ($\bigcirc$), and $T = 1.10$ ($\times$).

We have included our raw data in Table I to facilitate the work of others who venture into simulation of this model. We have found the results of Tobochnik and Chester,[19] Edwards,[15] Gupta *et al.*[23] and Wolff[14] of immeasurable benefit in this regard.

5. CONCLUSION

We have developed an efficient method of simulating the planar model where the update of a spin is only slightly longer than the update of a spin for the Ising model. This was achieved by selecting a new direction for the target spin from a list of deflection angles away from the direction of the resultant vector. This list was determined by the magnitude of the resultant vector and temperature; the angles occurred with a frequency proportional to their Boltzmann probabilities. This has allowed us to simulate the planar model on workstations with VAX 11/780 capabilities. The algorithm is fairly demanding of memory—an array of 640,000 elements is required to store the $\{\Theta$'s$\}$ for the direction update. Most of the computation was done on a DEC 3000 workstation with 16 Megabytes of memory.

We find that our results are compatible with the general tenets of the Kosterlitz–Thouless theory. At low temperatures ($T < 0.9$) the correlation exponent η is temperature dependent. We note that the spin-wave prediction for η agrees quite well with our numerical results for $T < 0.5$, when the presence of vortices begins to cause deviations from the predictions of spin-wave theory. The helicity modulus falls sharply but in a continuous manner in the vicinity of the KT transition; however, it is not hard to imagine a sharp discontinuity for the infinite system. The specific heat displays a peak extrapolated for an infinite system to be at a temperature of ~ 1.02 quite distinct from the KT transition temperature at ~ 0.9. The specific heat peak reflects the point at which the V/AV pairs are weakly bound. The maximum V/AV separation (where the pairs are for the first time weakly bound) occurs at a temperature consistent with the specific heat peak for all lattice sizes, confirming this explanation. The height of the specific heat peak appears to be independent of the size of the system for $L > 30$ and is therefore not associated with critical properties. The KT transition at $T \sim 0.9$ indicates the onset of the separation of the V/A pairs, whereas at a temperature above 1.0, the vortex is at a maximum distance from its neighboring antivortex. This is in accord with the KT picture.

ACKNOWLEDGMENTS

D.L.H. and N.J. are supported with NSERC grants and C.B. is the recipient of a summer undergraduate NSERC award. We thank A. B. MacIsaac, C. Liem, G. Corsten, A. Coniglio, and D. Stauffer for discussions and comments.

REFERENCES

1. J. M. Kosterlitz and D. J. Thouless, in *Progress in Low Temperature Physics*, Vol. VII(b), D. F. Brewer, ed. (North-Holland, Amsterdam, 1978).
2. P. Minnhagen, *Rev. Mod. Phys.* **59**:1001 (1987).
3. G. Corsten *et al.*, in *Correlations and Connectivity: Geometric Aspects of Physics, Chemistry and Biology*, H. E. Stanley and N. Ostrowsky, eds. (Kluwer Academic, 1990).
4. N. D. Mermin and H. Wagner, *Phys. Rev. Lett.* **17**:1133 (1966).
5. P. C. Hohenberg, *Phys. Rev.* **158**:383 (1967).
6. D. Jasnow and M. E. Fisher, *Phys. Rev. Lett.* **23**:286 (1969).
7. H. E. Stanley and T. A. Kaplan, *Phys. Rev. Lett.* **17**:913 (1966).
8. H. E. Stanley, *Phys. Rev. Lett.* **20**:589 (1968).
9. M. A. Moore, *Phys. Rev. Lett.* **23**:861 (1969).
10. H. E. Stanley, *Introduction to Phase Transitions and Critical Phenomena* (Oxford University Press, Oxford, 1971).
11. F. J. Wegner, *Z. Phys.* **206**:465 (1967).
12. V. L. Berezinskii, *Sov. Phys. JETP* **34**:610 (1971).
13. J. Jose, L. P. Kadanoff, S. Kirkpatrick, and D. R. Nelson, *Phys. Rev. B* **16**:1217 (1977).
14. U. Wolff, *Nucl. Phys. B* **300**[FS22]:501 (1988).
15. J. S. Wang and R. H. Swendsen, *Physica A* **167**:565 (1990), and references therein; R. G. Edwards, Ph.D. Thesis, New York University (1989).
16. J. M. Kosterlitz and D. J. Thouless, *J. Phys. C* **6**:1181 (1973).
17. J. M. Kosterlitz, *J. Phys. C* **7**:1046 (1974).
18. K. Binder, ed., *Applications of the Monte Carlo Method in Statistical Physics* (Springer-Verlag, Berlin, 1984).
19. J. Tobochnik and S. V. Chester, *Phys. Rev. B* **20**:3761 (1979).
20. C. Kawabata and K. Binder, *Solid State Commun.* **22**:705 (1977).
21. J. Kogut and J. Polonyi, *Nucl. Phys. B* **265**:313 (1986).
22. J. F. Fernandez, M. F. Ferreira, and J. Stankiewicz, *Phys. Rev. B* **34**:292 (1986).
23. R. Gupta, J. DeLapp, G. G. Batrouni, G. C. Fox, C. F. Baillie, and J. Apostolakis, *Phys. Rev. Lett.* **61**:1996 (1988).
24. A. M. Ferrenberg and R. H. Swendsen, *Phys. Rev. Lett.* **61**:2635 (1988).
25. P. B. Bowen *et al.*, *Phys. Rev. B* **40**:7439 (1989).
26. S. Teitel and C. Jayaprakash, *Phys. Rev. B* **27**:598 (1983).
27. A. Patrascioiu and E. Seiler, *Phys. Rev. Lett.* **60**:875 (1988).
28. S. Heinekamp and R. Pelcovits, *Phys. Rev. B* **32**:4528 (1985).